A nonlinear cascade model for action potential encoding in an insect sensory neuron

Andrew S. French* and Michael J. Korenberg‡
*Department of Physiology, University of Alberta, Edmonton, Alberta, T6G 2H7, Canada; and ‡Department of Electrical Engineering, Queen's University, Kingston, Ontario, K7L 3N6, Canada

ABSTRACT Action potential encoding in the cockroach tactile spine neuron can be represented as a single-input single-output nonlinear dynamic process. We have used a new functional expansion method to characterize the nonlinear behavior of the neural encoder. This method, which yields similar kernels to the Wiener method, is more accurate than the latter and is efficient enough to obtain reasonable kernels in less than 15 min using a personal computer. The input stimulus was band-limited white Gaussian noise and the output consisted of the resulting train of action potentials, which were unitized to give binary values. The kernels and the system input-output signals were used to identify a model for encoding comprising a cascade of dynamic linear, static nonlinear, and dynamic linear components. The two dynamic linear components had repeatable and distinctive forms with the first being low-pass and the second being high-pass. The static nonlinearity was fitted with a fifth-order polynomial function over several input amplitude ranges and had the form of a half-wave rectifier. The complete model gave a good approximation to the output of the neuron when both were subjected to the same novel white noise input signal.

INTRODUCTION

Action potential encoding from membrane current fluctuations in neurons has been represented by a wide range of models (Perkel and Bullock, 1968; Holden, 1976). These models vary from purely empirical forms, which attempt to mimic behavior independently of neuronal anatomy or physiology, to analogues which represent the actual ionic currents and channels as closely as possible (Hodgkin and Huxley, 1952). For some interesting neurons, it is difficult to characterize the ionic currents underlying action potential encoding, but it is possible to measure their input-output relationships. Linear systems analysis has been widely used to characterize the input-output characteristics of neural encoders (Stein et al., 1972) and this approach can be used to produce models of encoding which are combinations of simple linear components. However, neural encoders often show strongly nonlinear behavior such as rectification or saturation so that nonlinear systems analysis is required to obtain models intended to represent these nonlinearities.

Sensory neurons perform the first steps in signal acquisition and processing by nervous systems, and their inputs may often be carefully controlled by the experiment to allow the input and output signals to be single valued functions of time. White noise analysis techniques have been used in attempts to model nonlinear information coding in several sensory systems (Marmarelis and Naka, 1972; French and Wong, 1977; Marmarelis and Marmarelis, 1978). These investigations used the cross-correlation method suggested by Lee and Schetzen (1965), or a similar frequency domain approach (French and Butz, 1973) to obtain the Wiener kernels of the system (Wiener, 1958).

In practice, these methods often give inaccurate system identification (Palm and Poggio, 1978) partly because it is experimentally impossible to provide stimuli of infinite duration or bandwidth, and unlimited amplitude. The data analysis procedures are also very time consuming. To overcome these problems and achieve greater accuracy, a new fast orthogonal method has been developed for estimating nonlinear system kernels (Korenberg, 1988). This method does not require the input signal to be white, Gaussian, or of infinite duration, but implicitly creates a set of functionals which are orthogonal for the given input. Consequently, accurate kernel estimates can be obtained from much shorter data records. The kernel estimates generally depend upon the input signal because the estimates minimize the mean-square error between the system and the functional series outputs, for the particular input signal used. If this signal is approximately Gaussian white noise, then the kernels of the functionals are good approximations to the Wiener kernels. This method is efficient enough to allow small personal computers to be used for nonlinear system identification.

The cockroach tactile spine is an example of a primary sensory neuron, in which the input is movement of the spine and the output is a series of action potentials. This preparation was one of the first sensory systems to be used for quantitative analysis of sensory coding via the linear frequency response function (Pringle and Wilson, 1952; Chapman and Smith, 1963), but the tactile spine shows the nonlinearities of rectification and phase-locking to

0006-3495/89/04/655/07 $2.00

repetitive stimuli (French et al., 1972). Recently, we have shown that the dynamic properties of the tactile spine neuron are dominated by the encoding stage (French, 1984). This allows the use of a reduced preparation in which controlled electric current is applied directly to the membrane of the sensory neuron to elicit action potentials.

We have previously demonstrated the utility of the fast orthogonal method using the tactile spine neuron as a nonlinear system at low temporal resolution (Korenberg et al., 1988). We have now used the same method to examine nonlinear behavior in the tactile spine encoder at much higher temporal resolution and find that the encoder can be well approximated by a cascade of dynamic linear, static nonlinear, and dynamic linear elements.

METHODS

Experiments were performed on tactile spines from metathoracic legs of adult cockroaches, *periplaneta americana*. The experimental arrangement for stimulating the tactile spine neuron and recording the resulting action potentials is shown in Fig. 1. This preparation has been described in detail before (French, 1984). The input signal was obtained from a pseudorandom binary sequence with a clock frequency of 1 kHz and band-limited to 0–250 Hz by a nine-pole active analogue filter. The noise signal drove a constant voltage-to-current converter which, in turn, stimulated the neuron. The stimulus current was monitored by a current detector in the ground return circuit. The input signal was sampled at 2-ms intervals by a 12-bit analogue-to-digital converter. Action potentials were detected by a Schmitt trigger and used to construct a unitized output signal at 2-ms intervals consisting of values of 1 when an action potential had occurred within the interval, and 0 at all other times (Sakuranaga et al., 1987).

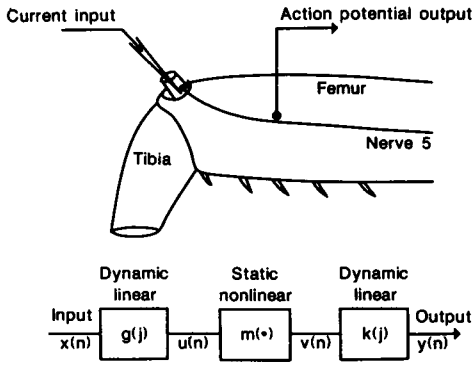

FIGURE 1. The experimental preparation for stimulating the tactile spine neuron and recording the resulting action potentials (*top*). A controlled current was applied extracellularly to the action potential–initiating region of the neuron through the amputated spine lumen. Action potentials were recorded extracellularly from the afferent nerve ~3 mm along the femur. Stimulus current was the input, $x(n)$, to the nonlinear cascade model (*bottom*), whereas action potentials were the output, $y(n)$.

The experimental record was divided into sections of 15,000 pairs of input, $x(n)$, and output, $y(n)$, values. These sections were then analyzed by the fast orthogonal algorithm which we have described in detail before (Korenberg, 1988; Korenberg et al., 1988). The nonlinear dynamic model of the system was first approximated by:

$$y_s(n) = h_0 + \sum_{j=0}^{M} h_1(j)x(n-j) + \sum_{j_1=0}^{M}\sum_{j_2=0}^{M} h_2(j_1,j_2)x(n-j_1)x(n-j_2), \quad (1)$$

where the zero-, first-, and symmetric second-order kernels are h_0, $h_1(j)$, and $h_2(j_1, j_2)$, respectively, and the system memory is assumed to last up to a maximum input lag of M. The fast orthogonal algorithm selects the kernels to minimize the mean-square error:

$$e = \overline{[y(n) - y_s(n)]^2}, \quad (2)$$

where the bar indicates a time average over the entire record length of $x(n)$, $y(n)$. In these experiments a kernel memory length of 17 lags was used, yielding kernels with $j, j_1, j_2 = 0$–16.

Because the input signal in the experiments closely resembled Gaussian white noise, the kernel estimates approximated Wiener kernels of corresponding order. This enabled us to approximate the system behavior by a nonlinear cascade structure as shown in Fig. 1. This model consists of a first dynamic linear component with impulse response $g(j)$, a static nonlinearity $m(\cdot)$, and a second dynamic linear component with impulse response $k(j)$. (The term "impulse response" is used for reasons of familiarity, but the term "delta response" would be more accurate because the model is defined in discrete time rather than continuous time.) The impulse response of the first linear component, $g(j)$, was obtained from a slice through the second-order kernel, because it can be shown that $g(j)$ is proportional to $h_2(j, 0)$ provided that the latter is not identically zero (Korenberg, 1982, 1985). The impulse response of the second linear component, $k(j)$, was obtained by deconvolving $h_1(j)$ with $g(j)$, because for the cascade model, $h_1(j)$ is proportional to a convolution of the impulse responses of the two linear components (Bussgang, 1952; Spekreijse and Oosting, 1970; Korenberg et al., 1988). Two methods of performing the deconvolution were tested, an iterative discrete time domain algorithm, and division of the Fourier transforms followed by inverse Fourier transformation of the quotient. The two methods gave identical results under most conditions but the time domain method occasionally became unstable. The results presented here were all obtained by the frequency domain method.

A test of the ability of the cascade model to account for the overall behavior is to synthesize the second-order kernel from the two linear components, because the model (Korenberg, 1973*a* and *b*) predicts that

$$h_2(j_1, j_2) = C_1 \sum_{r=0}^{M} k(r)g(j_1 - r)g(j_2 - r), \quad (3)$$

where C_1 is a constant. This prediction was tested for all experiments. Note that only a single slice of the experimental second-order kernel is required to identify the linear components, whereas Eq. 3 may be used to predict the entire second-order kernel. The static nonlinearity, $m(\cdot)$, was approximated by a polynomial series:

$$m(\cdot) = \sum_{i=0}^{I} a_i(\cdot)^i, \quad (4)$$

where a_i are the polynomial coefficients. The coefficients were estimated from the impulse responses of the two linear components and the entire 15,000 pairs of experimental data, using a minimum square error procedure (Korenberg et al., 1988). A fifth-order polynomial approximation was used in all experiments.

The above method identifies the two dynamic linear components in the time domain. Then, the frequency response functions of the linear components can be obtained directly from the Fourier transforms of $g(j)$ and $k(j)$. However, an alternative means of obtaining the gain portions of these frequency response functions is via the Fourier transforms of the first- and second-order kernels (Korenberg, 1973*a* and *b*):

$$|G(\omega)| = C_2|H_2(-\omega/2, \omega)|/|H_1(\omega/2)| \quad (5)$$

$$|K(\omega)| = C_3|H_1(\omega)|/|G(\omega)|, \quad (6)$$

where $K(\omega)$, $H_1(\omega)$, and $G(\omega)$ are the Fourier transforms of the respective time-domain variables, $k(j)$, $h_1(j)$, and $g(j)$, ω is frequency, and C_2 and C_3 are constants. This method has the advantage of using the entire first- and second-order kernels to compute the gains of the two linear components and might therefore be expected to be more accurate. In practice, the two methods gave similar results, with the frequency domain values being slightly smoother than those obtained from Fourier transforming the impulse responses identified in the time domain. Results shown here are from the frequency domain method (Eqs. 5 and 6).

RESULTS

First-order kernels, $h_1(j)$, from three tactile spine experiments are shown in Fig. 2. Two of the kernels, *B* and *C*, were obtained from consecutive sets of 15,000 input-output pairs during an experiment with input root-mean-square current amplitude 10.98 nA. The other two kernels, *A* and *D*, were obtained from experiments on the same preparation with input amplitudes of 4.85 and 20.2 nA, respectively. The letters, *A–D*, refer to the same four data sets throughout. The two kernels obtained from different sections of the same data set were very similar. This was a consistent finding, and indicates that the method gives reliable and reproducible results, as well as showing that the preparation is stable during long periods of stimulation. With higher stimulus amplitudes the first-order kernel had significantly more negative excursion after the initial positive peak, suggesting less damped behavior. A total of nine experiments were conducted on three different tactile spine neurons. The first-order kernels shown here were found reproducibly in all these experiments. The forms of the kernels beyond ~10 ms lag were not reproducible and must be considered to be due to random fluctuations around zero. The rapid transitions at the beginning of the first-order kernel suggest that additional information might be gained from a higher sampling rate in future work.

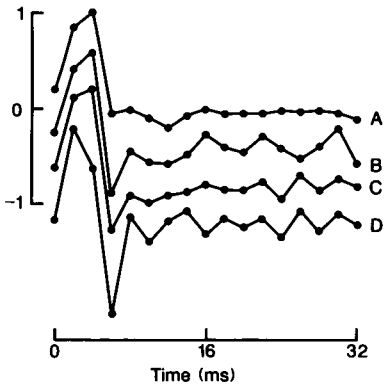

FIGURE 2 First-order kernels, $h_1(j)$, obtained from tactile spine stimulation experiments. Two traces show measurements from contiguous sets of data during an experiment with an input root-mean-square current amplitude of 10.98 nA (traces *B* and *C*). The other measurements were obtained with stimulus currents of 4.85 nA (*A*) and 20.2 nA (*D*). All traces have been normalized to a maximum positive excursion of 1. Traces *B–D* have been shifted downwards for clarity. All traces reached final values of approximately zero. The same data sets are referred to in subsequent figures.

A perspective plot of the second order kernel, $h_2(j_1, j_2)$, obtained from data set *C* is shown in Fig. 3. The peak of the kernel was at $h_2(0, 0)$ and the flat plane at maximum lags had a mean of approximately zero. The kernel is shown after rotations of 70° in the yaw plane and 20° in the pitch plane. This data was smoothed by averaging each point with its immediate neighbors before plotting. Smoothing was used only to improve the visual appearance of the kernels and did not affect their general forms. Second-order kernels with similar forms were obtained from the same experiments as were described above for the first-order kernel.

Estimates of the impulse response of the first linear component, $g(j)$, extracted from the second-order kernels are shown in Fig. 4. This component was of low-pass form with significant structure to ~16 ms lag. The form of the component was similar in each case, but again showed increasingly negative excursions at higher input amplitudes. Our previous experiments as much lower temporal resolution gave a first linear component which was so brief that it was difficult to distinguish it from a discrete

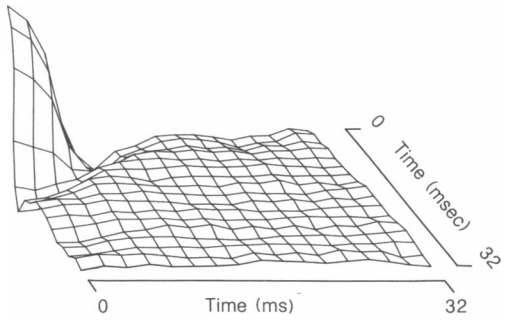

FIGURE 3 The second-order kernel, $h_2(j_1, j_2)$, obtained from the same data set as trace *C* in Fig. 2.

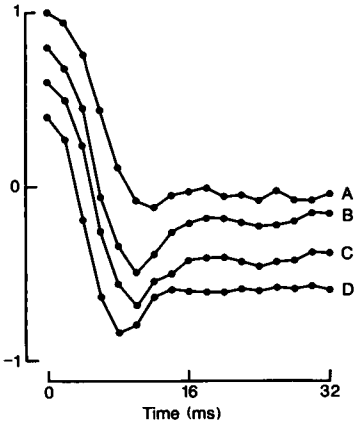

FIGURE 4 The first dynamic linear component of the cascade, $g(j)$, for the same four experiments as Fig. 2. Traces *B* and *C* show measurements from contiguous sets of data during an experiment with an input root-mean-square amplitude of 10.98 nA. Other traces were obtained with stimuli of 4.85 nA (*A*) and 20.2 nA (*D*). All traces have been normalized to give an absolute excursion of ±1. Traces *B–D* have been shifted downwards for clarity. All traces reached final values of approximately zero.

time impulse, i.e., a delta function (Korenberg et al., 1988). However, the present results demonstrate that an initial linear dynamic component is required to account for the behavior of the tactile spine neuron.

Estimates of the impulse response of the second linear component, $k(j)$, obtained by deconvolution from the first-order kernel, are shown in Fig. 5. This component also had a much more clearly defined structure than we were able to obtain previously and showed high-pass characteristics. Increasing input amplitude in this case again led to more underdamped behavior.

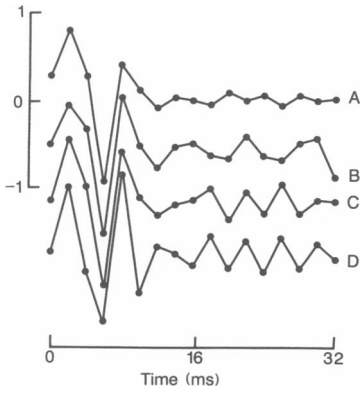

FIGURE 5 The second dynamic linear component of the cascade, $k(j)$, for the same four experiments as Fig. 2. In this case the traces were normalized to a maximum negative excursion of −1. Traces *B–D* have been shifted downwards for clarity.

Fig. 6 shows Bode plots of the gains of the frequency response functions of the two linear components obtained from Eqs. 5 and 6 using the Fourier transforms of the unsmoothed kernels from data set *C*. The first component, $|G(\omega)|$, was low-pass as expected from the impulse response, and was well fitted by a critically damped second-order pole with corner frequency 62 Hz. The second component, $|K(\omega)|$, was high-pass but of more complex form. There was not a clear asymptote at low frequency, and the ascending response did not follow a clear first- or second-order slope. The second component appeared to have an initial corner frequency of ~40 Hz, which would lead to a high-pass response overall. This agrees with the experimental results from frequency response measurements on this preparation (French et al., 1972; French and Kuster, 1981). Because of the unusual form of the gain plot of the second linear component, we intend to perform a spectral analysis of the impulse responses of Fig. 5 using a fast orthogonal search (Korenberg, 1987). This technique can be used to discover the most significant frequencies in the time-series data, and is more accurate than conventional Fourier series analysis. Gain plots similar to those of Fig. 6 were also obtained from Fourier transforming the first and second linear components of Figs. 4 and 5. This agreement between gain plots from two different estimation methods provides additional support for the cascade model.

Estimates of the static nonlinear component in the cascade, $m(\cdot)$, from the same four experiments are shown in Fig. 7. These were approximated by a fifth-order

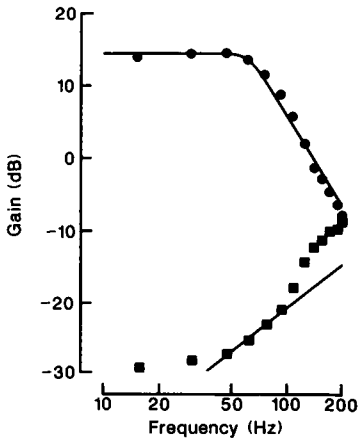

FIGURE 6 Bode plots of the gain portions of the frequency response functions of the two dynamic linear components, $|G(\omega)|$ (*circles*) and $|K(\omega)|$ (*squares*), for experiment *C*. These data were obtained from Eqs. 5 and 6 using Fourier transforms of the first- and second-order kernels. Solid lines are fitted by eye. For the upper trace the slopes are 0 and −40 dB per decade. For the lower trace a slope of 20 dB per decade is fitted to part of the response.

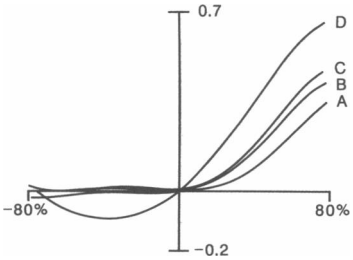

FIGURE 7 The static nonlinear component, $m(\cdot)$, for the four experiments of Fig. 2. In each case the response has been normalized to 80% of the amplitude range at the input to the static nonlinearity, because a Gaussian signal contains relatively little power at large excursions and the estimates of $m(\cdot)$ were unreliable at the extreme input amplitudes.

polynomial over the range of maximum excursions calculated for the input to the static nonlinearity during the experiments. The static nonlinearity closely approximated a half-wave rectifier which passes only positive, or depolarizing, inputs. This result was reproducible between experiments and preparations.

Fig. 8 shows the second-order kernel predicted by the nonlinear cascade of Fig. 1 using Eq. 3 and the two linear components, $g(j)$ and $k(j)$, from experiment *C*. This prediction should be compared with Fig. 3. As a further test of the cascade model (Fig. 1), the output of the cascade was calculated in response to input signals from the same experiments but from different sections than were used to obtain the kernels. This allowed a direct comparison between the predicted output of the model and the actual output from the receptor neuron. Fig. 9 shows a short section of such a comparison chosen at random from the data. It can be seen that the model output (lower) had a spiky appearance and the peaks corresponded very well with the experimental action

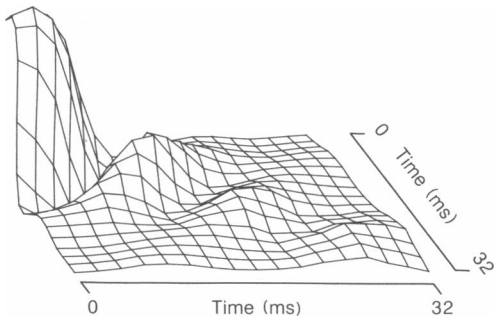

FIGURE 8 A simulated second-order kernel obtained from the two dynamic linear components, $g(j)$ and $k(j)$, of experiment C and Eq. 3. This should be compared with the experimental second-order kernel of Fig. 3.

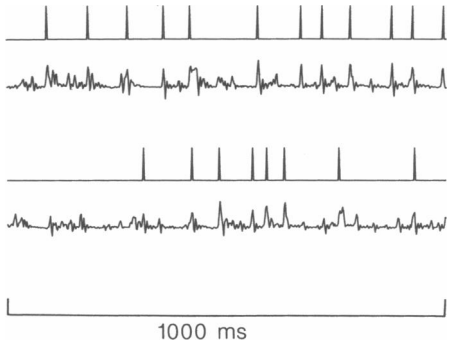

FIGURE 9 Comparison of output signals from the neuron (*top*) and the nonlinear cascade (*bottom*) using the linear and nonlinear components of experiment C. The lower pair of traces is a continuation of the upper pair, showing a total period of 2 s. The input noise and action potential output were taken from another section of the same experimental data, but not from the data which had been used to obtain the kernels.

potentials, although the agreement was not perfect. In our earlier work (Korenberg et al., 1988) with lower temporal resolution, we used a threshold to select the predicted positions of action potentials. This was hardly necessary with the improved resolution of the present experiments but a suitable threshold applied to the model output would predict the experimental output with spike error rate of ~20% (false positives and negatives).

DISCUSSION

The results indicate that the nonlinear cascade of Fig. 1 provides a reasonable model of action potential encoding in this sensory neuron. The second-order kernel predicted from the cascade (Fig. 8) is not a perfect replica of the experimentally derived kernel (Fig. 3) but it has the same general form. Similarly, the output of the cascade to a novel input (Fig. 9) is not a perfect replica of the actual neural output, but predicts the action potentials quite faithfully. A more complex system with additional nonlinear and linear components in series or parallel with the present cascade would probably provide a more accurate model of encoding, but the simple cascade of Fig. 1 provides a good initial approximation.

Before the availability of the fast orthogonal algorithm for investigating nonlinear dynamic systems, we attempted to identify the major linear and nonlinear components in insect sensory receptors by Wiener kernel analysis in the frequency domain (French and Butz, 1973). In the case of cockroach hair plate receptors, which have different dynamic properties to the tactile spine, we found that the behavior could best be explained by a dynamic linear component followed by a static

nonlinearity (French and Wong, 1977). In the case of the tactile spine neuron, we found it more difficult to decide if the major dynamic linear component was before or after a static nonlinearity (French, 1980). The present results make this puzzle more comprehensible, because the new model requires significant dynamic linear components both before and after the static nonlinearity.

In our earlier investigation of this system, using much lower temporal resolution, we could not be certain that the first dynamic linear component was required to describe the behavior (Korenberg et al., 1988) but the present results make it clear that this component is required and has a very different form to the second linear component. The additional structure obtained in both linear components provides sufficient information to begin interpreting the nonlinear model in terms of physical components of the neuron.

The finding that the static nonlinearity is a half-wave rectifier confirms our previous findings on the form of nonlinearity in this receptor (French, 1980). This is reflected in the overt behavior of the receptor, which does not respond to hyperpolarizing stimuli, but responds strongly to depolarizing inputs. The underlying cause of this response presumably lies in the voltage sensitivity of sodium channels in the neural membrane, which are activated only by depolarizing stimuli. There is only slight evidence of saturation in the nonlinear component, indicating that the encoder can function relatively linearly over a wide range of depolarizing input currents.

The linear frequency response function of the tactile spine neuron has been studied under a wide range of conditions (French et al., 1972; French and Kuster, 1981). The form of the frequency response is high-pass over the range 0–500 Hz with a fractional power-law relationship between gain and frequency. The phase relationship is also well fitted by the fractional power-law model with an additional delay component of ~1.5 ms, due to the conduction of action potentials from the nerve cell body to the recording site along the axon. Because the delay is the last component it should in reality be present in the second linear component of the cascade model. However, moving a pure time delay from one linear component to the other does not change the input-output behavior of the cascade. In our analysis the delay did appear in the second linear component because the component is close to zero at zero time (Fig. 5), but the temporal resolution of 2 ms was not adequate to resolve the delay accurately. The second linear component also seems to control the high-pass response of the neuron. The cause of this high-pass behavior is not known, but is possibly due to a slow inactivation of sodium channels (French, 1987). It would therefore occur after sodium channel activation, as indicated by its position after the rectifier in the cascade.

The physical basis of the first linear component is harder to identify. Current injected into the neuron should be shunted by the membrane capacitance and this would be expected to give a low-pass response. However, all estimates of the membrane time constant in this neuron give values of ~1 ms (French, 1987), which is faster than the response in Fig. 4. The frequency response of the first component (Fig. 6) gives a time constant of ~2.5 ms but it is also second-order, indicating that more than a single time constant is involved. The input current could be shunted by an additional conductance, most likely potassium or chloride, which is activated by depolarization with a slower time constant. There is no direct evidence for any major conductance with a time constant in this range, but voltage clamp experiments have not yet been possible on this neuron. The combination of such an additional conductance with the membrane time constant might then account for the second-order behavior. Both the dynamic linear components became less damped with greater input signal amplitudes, which could be due to the increased involvement of voltage-activated conductances in shunting the stimulus current and controlling the threshold for action potentials.

Although nonlinear systems analysis cannot provide direct measurements of the ionic currents underlying action potential encoding, it promises to be a useful adjunct approach to conventional biophysical experiments, especially for neurons which are experimentally intractable. The application of Wiener kernel analysis to this type of system was not really feasible before the fast orthogonal algorithm, with its significantly greater accuracy, became available. It should now be possible to construct realistic biophysical models of encoder processes, using ionic channels and other membrane components, and to identify the nonlinear dynamic properties of such models for comparison with known neuronal behavior.

We thank Rodney Gramlich for expert technical assistance, and two anonymous referees for valuable suggestions to improve the manuscript.

Support for this work was provided by the Medical Research Council of Canada, the Natural Sciences and Engineering Research Council of Canada, the Advisory Research Committee of Queen's University, and the Alberta Heritage Foundation for Medical Research.

Received for publication 11 July 1988 and in final form 9 December 1988.

REFERENCES

Bussgang, J. J. 1952. Crosscorrelation functions of amplitude-distorted Gaussian signals. *MIT Res. Lab. Elec. Tech. Rep.* 216:1–14.

Chapman, K. M. and R. S. Smith. 1963. A linear transfer function underlying impulse frequency modulation in a cockroach mechanoreceptor. *Nature* (*Lond.*) 197:699–700.

French, A. S. 1980. Sensory transduction in an insect mechanoreceptor: linear and nonlinear properties. *Biol. Cybern.* 38:115–123.

French, A. S. 1984. Dynamic properties of the action potential encoder in an insect mechanosensory neuron. *Biophys. J.* 46:285–290.

French, A. S. 1987. Removal of rapid adaptation from an insect mechanoreceptor neuron by oxidizing agents which affect sodium channel inactivation. *J. Comp. Physiol.* A161:275–282.

French, A. S., and E. G. Butz. 1973. Measuring the Wiener kernels of a nonlinear system using the fast Fourier transform. *Int. J. Control.* 17:529–539.

French, A. S., and J. E. Kuster. 1981. Sensory transduction in an insect mechanoreceptor: extended bandwidth measurements and sensitivity to stimulus strength. *Biol. Cybern.* 42:87–94.

French, A. S., and R. K. S. Wong. 1977. Nonlinear analysis of sensory transduction in an insect mechanoreceptor. *Biol. Cybern.* 26:231–240.

French, A. S., A. V. Holden, and R. B. Stein. 1972. The estimation of the frequency response function of an insect mechanoreceptor. *Kybernetik.* 11:15–23.

Hodgkin, A. L., and A. F. Huxley. 1952. A quantitative description of membrane current and its application to conduction and excitation in nerve. *J. Physiol.* (*Lond.*). 117:500–544.

Holden, A. V. 1976. Models of the Stochastic Activity of Neurones. Springer-Verlag, New York. 368 pp.

Korenberg, M. J. 1973*a*. Identification of biological cascades of linear and static nonlinear systems. *Proc. 16th Midwest Symp. Circuit Theory.* 18.2:1–9.

Korenberg, M. J. 1973*b*. Cross-correlation analysis of neural cascades. *Proc. 10th Annu. Rocky Mountain Bioeng. Symp.* 47–52.

Korenberg, M. J. 1982. Statistical identification of parallel cascades of linear and nonlinear systems. *In* International Federation of Automatic Control Symposium on Identification of Systems and Parameter Estimation. 580–585.

Korenberg, M. J. 1985. Identifying noisy cascades of linear and static nonlinear systems. *In* International Federation of Automatic Control Symposium on Identification of Systems and Parameter Estimation. 421–426.

Korenberg, M. J. 1987. Fast orthogonal identification of nonlinear difference equation and functional expansion models. *Proc. 30th Midwest Symp. Circuit Sys.* 1:270–276.

Korenberg, M. J. 1988. Identifying nonlinear difference equation and functional expansion representations: the fast orthogonal algorithm. *Ann. Biomed. Eng.* 16:123–142.

Korenberg, M. J., A. S. French, and S. K. L. Voo. 1988. White-noise analysis of nonlinear behavior in an insect sensory neuron: kernel and cascade approaches. *Biol. Cybern.* 58:313–320.

Lee, Y. W., and M. Schetzen. 1965. Measurement of the Wiener kernels of a nonlinear system by cross-correlation. *Int. J. Control.* 2:237–254.

Marmarelis, P. Z., and V. Z. Marmarelis. 1978. Analysis of Physiological Systems: The White Noise Approach. Plenum Publishing Corp., New York. 487 pp.

Marmarelis, P. Z., and K.-I. Naka. 1972. White noise analysis of a neuron chain: an application of the Wiener theory. *Science* (*Wash. DC*). 175:1276–1278.

Palm, G., and T. Poggio. 1978. Stochastic identification methods for nonlinear systems: an extension of the Wiener theory. *SIAM* (*Soc. Ind. Appl. Math.*) *J. Appl. Math.* 34:524–534.

Perkel, D. H., and T. H. Bullock. 1968. Neural coding. *Neurosci. Res. Prog. Bull.* 6:221–348.

Pringle, J. W., and V. J. Wilson. 1952. The response of a sense organ to a harmonic stimulus. *J. Exp. Biol.* 29:220–234.

Sakuranaga, M., Y.-I. Ando, and K.-I. Naka. 1987. Dynamics of ganglion cell response in the catfish and frog retinas. *J. Gen. Physiol.* 90:229–259.

Spekreijse, H., and J. Oosting. 1970. Linearizing: A method for analysing and synthesizing nonlinear systems. *Kybernetik.* 7:23–31.

Stein, R. B., A. S. French, and A. V. Holden. 1972. The frequency response, coherence, and information capacity of two neuronal models. *Biophys. J.* 12:295–322.

Wiener, N. 1958. Nonlinear Problems in Random Theory. John Wiley and Sons, New York. 131 pp.